



HAL
open science

In vivo effector functions of high-affinity mouse IgG receptor Fc γ RI in disease and therapy models

Caitlin M. Gillis, Priscila P. Zenatti, David A. Mancardi, Héloïse Beutier, Laurence Fiette, Lynn E. Macdonald, Andrew J. Murphy, Susanna Celli, Philippe Bouso, Friederike Jönsson, et al.

► To cite this version:

Caitlin M. Gillis, Priscila P. Zenatti, David A. Mancardi, Héloïse Beutier, Laurence Fiette, et al.. In vivo effector functions of high-affinity mouse IgG receptor Fc γ RI in disease and therapy models. *Journal of Autoimmunity*, 2017, 80, pp.95-102. 10.1016/j.jaut.2016.09.009 . pasteur-01388794

HAL Id: pasteur-01388794

<https://pasteur.hal.science/pasteur-01388794>

Submitted on 27 Oct 2016

HAL is a multi-disciplinary open access archive for the deposit and dissemination of scientific research documents, whether they are published or not. The documents may come from teaching and research institutions in France or abroad, or from public or private research centers.

L'archive ouverte pluridisciplinaire **HAL**, est destinée au dépôt et à la diffusion de documents scientifiques de niveau recherche, publiés ou non, émanant des établissements d'enseignement et de recherche français ou étrangers, des laboratoires publics ou privés.



Distributed under a Creative Commons Attribution - NonCommercial 4.0 International License

In vivo effector functions of high-affinity mouse IgG receptor FcγRI in disease and therapy models

Caitlin M. Gillis^{1,2,3}, Priscila P. Zenatti^{1,2}, David A. Mancardi^{1,2}, Héloïse Beutier^{1,2,3}, Laurence Fiette⁴, Lynn E. Macdonald⁵, Andrew J. Murphy⁵, Susanna Celli^{6,7}, Philippe Bousso^{6,7},
Friederike Jönsson^{1,2} and Pierre Bruhns^{1,2}

Authors' affiliations

¹Institut Pasteur, Department of Immunology, Unit of Antibodies in Therapy and Pathology, Paris, France;

²INSERM, U1222, Paris, France;

³Université Pierre et Marie Curie, Paris, France;

⁴Département Infection et Epidémiologie, Unité d'Histopathologie Humaine et Modèles Animaux, Institut Pasteur, Paris, France;

⁵Regeneron Pharmaceuticals, Inc., Tarrytown, NY, USA;

⁶Institut Pasteur, Dynamics of Immune Responses Unit, 75015 Paris, France;

⁷INSERM U1223, rue du Dr Roux, Paris, France.

Sources of funding: none of the sources of funding have an interest in the subject matter or materials discussed in the submitted manuscript

Correspondence to: Pierre Bruhns, Unit of Antibodies in Therapy and Pathology, INSERM U1222, Department of Immunology, Institut Pasteur, 25 rue du Docteur Roux, 75015 Paris, France. Phone: +33145688629. E-mail: bruhns@pasteur.fr

ABSTRACT

Two activating mouse IgG receptors (FcγRs) have the ability to bind monomeric IgG, the high-affinity mouse FcγRI and FcγRIV. Despite high circulating levels of IgG, reports using FcγRI^{-/-} or FcγRIV^{-/-} mice or FcγRIV-blocking antibodies implicate these receptors in IgG-induced disease severity or therapeutic Ab efficacy. From these studies, however, one cannot conclude on the effector capabilities of a given receptor, because different activating FcγRs possess redundant properties *in vivo*, and cooperation between FcγRs may occur, or priming phenomena. To help resolve these uncertainties, we used mice expressing only FcγRI to determine its intrinsic properties *in vivo*. FcγRI^{only} mice were sensitive to IgG-induced autoimmune thrombocytopenia and anti-CD20 and anti-tumour immunotherapy, but resistant to IgG-induced autoimmune arthritis, anaphylaxis and airway inflammation. Our results show that the *in vivo* roles of FcγRI are more restricted than initially reported using FcγRI^{-/-} mice, but confirm effector capabilities for this high-affinity IgG receptor *in vivo*.

1. INTRODUCTION

1
2
3 IgG receptors (Fc γ R) in both humans and mice are divided into high-affinity IgG
4 receptors that are able to retain monomeric IgG, and low-affinity IgG receptors that do not. Both
5 high- and low-affinity Fc γ Rs are, however, able to bind to IgG-immune complexes or IgG-
6 opsonised cells and surfaces. In humans only hFc γ RI is a high-affinity IgG receptor, for human
7 IgG1, IgG3 and IgG4; and in mice both mFc γ RI (for mouse IgG2a) and mFc γ RIV (for mouse
8 IgG2a and IgG2b) are high-affinity receptors [1]. Although it was proposed that high-affinity
9 Fc γ Rs are occupied by circulating IgG *in vivo* (discussed in [2]), multiple effector roles for
10 hFc γ RI, mFc γ RI and mFc γ RIV have been reported using mouse models of disease and therapy
11 [3-6].

12 hFc γ RI has been studied by exogenous expression in hFc γ RI^{tg} mice, demonstrating its
13 role on dendritic cells in the enhancement of antigen presentation and cross-presentation [7], and
14 on neutrophils and monocyte/macrophages in inflammation, autoimmunity and systemic
15 anaphylaxis [8]. These studies indicate that hFc γ RI can, by itself, induce clinical signs of
16 autoimmune diseases, by triggering local inflammation (*e.g.* autoimmune rheumatoid arthritis) or
17 phagocytosis (*e.g.* autoimmune thrombocytopenia and anaemia [9]). Additionally, hFc γ RI was
18 reported to induce allergic shock (anaphylaxis) triggered by IgG-immune complexes [8]. Finally,
19 hFc γ RI may also be a therapeutic target as it can mediate antibody-based therapies such as anti-
20 malaria [10], anti-metastatic melanoma [8] and angiogenesis prevention [6]. The mouse
21 counterpart of hFc γ RI, mFc γ RI, has been so far studied only by the effect of its absence.
22 Compared to wild-type, mFc γ RI^{-/-} mice demonstrate reduced reaction severity in models of
23 autoimmune diseases such as experimental haemolytic anaemia and arthritis [11, 12]. In addition

24 mFcγRI^{-/-} mice are less susceptible to IgG-mediated systemic anaphylaxis, Arthus reactions [13,
25 14], and show reduced efficacy of anti-melanoma [15-17], anti-lymphoma [18] and anti-
26 angiogenic therapies [6]. mFcγRIV was also initially studied by its absence in mFcγRIV^{-/-} mice
27 or by using blocking anti-mFcγRIV mAbs. These studies reported reduced IgG-mediated
28 autoimmune anaemia, thrombocytopenia, rheumatoid arthritis and experimental nephrotoxic
29 nephritis, but also reduced anaphylaxis and less efficient subcutaneous melanoma therapy in the
30 absence or after blockade of mFcγRIV [19, 20]; some of the latter results should be taken with
31 caution since mFcγRIV-blocking antibody 9E9 may also block mFcγRIII *in vivo* [21]. Effector
32 functions could nevertheless be definitively attributed to mFcγRIV through the generation of
33 mice expressing mFcγRIV without other FcγR. Indeed, using mFcγRIV^{only} mice we could
34 demonstrate that mFcγRIV can individually induce autoimmune thrombocytopenia and
35 rheumatoid arthritis, as well as IgG-mediated airway inflammation and anaphylaxis, but not anti-
36 metastatic melanoma therapy [8, 22-24]. Altogether these data propose multiple effector
37 functions for high-affinity receptors hFcγRI, mFcγRI and mFcγRIV in autoimmune and
38 inflammatory disease models, and therapy, with direct evidence provided by studies using
39 hFcγRI^{tg} mice and mFcγRIV^{only} mice, but only indirect evidence provided by mFcγRI^{-/-} mice.

40 The *in vivo* effector functions proposed for mFcγRI in IgG-mediated autoimmune disease
41 and therapy models are surprising, considering its expression is restricted to monocytes,
42 monocyte-derived dendritic cells and some tissue-resident macrophages, and is absent on
43 neutrophils. As several reports suggest redundant functions among mFcγRs (reviewed in [1, 2]),
44 it is uncertain if mFcγRI can induce IgG-mediated autoimmune diseases and therapeutic efficacy
45 by itself, or if this receptor is indirectly involved: either for optimal activation via other mFcγRs
46 or priming of effector cells. Therefore we analysed the *in vivo* effector functions of mFcγRI in

47 mFcγRI^{only} mice, *i.e.* in the absence of mFcγRIIB, mFcγRIII and mFcγRIV, in comparison with
48 mFcγR^{null} mice that express no mFcγR. Our results identify the effector functions of mFcγRI as
49 more restricted than initially reported, but confirm that mFcγRI does function independently *in*
50 *vivo*, in particular for depletion of IgG-opsonised cells.

51

2. MATERIALS & METHODS

52

53 2.1 Mice

54 C57BL/6J mice (WT) were purchased from Charles River. VG1505 (FcγRI^{only}) mice were
55 reported previously [17] and generated by Regeneron Pharmaceuticals, Inc. FcγR^{null} mice were
56 generated by crossing FcγRI^{only} mice to FcγRI^{-/-} mice. FcγRI^{only} and FcγR^{null} mice were bred at
57 Institut Pasteur, used for experiments at 8-11 weeks of age and all protocols were approved by
58 the Animal Ethics committee CETEA (Institut Pasteur, Paris, France) registered under #C2EA-
59 89.

60

61 2.2 K/BxN serum-induced passive arthritis

62 K/BxN serum was generated from a pooled collection of >40 animals. Arthritis was induced by
63 i.v. transfer of indicated volumes of K/BxN serum, and scored as described [25]. In some
64 experiments mice were sacrificed on day 8 for blinded histological assessment.

65

66 2.3 Airway Inflammation

67 As previously described [26], mice were injected with 50 μL of rabbit anti-OVA serum i.n. and
68 500 μg of OVA i.v. 16-18h later 4 bronchoalveolar lavages (BALs) were performed with cold
69 PBS (1x 0.5ml, then 3x 1mL) under lethal anaesthetic. Cells were pooled and stained for flow
70 cytometry after RBC lysis; and haemorrhage was determined by OD570nm in the supernatant.
71 We confirmed that mFcγRI, like all mouse FcγR, can indeed bind rabbit IgG immune complexes
72 (Supplementary Fig.2).

73

74 **2.4 Passive Systemic Anaphylaxis (PSA)**

75 Mice were sensitised by i.v. injection of 500µg anti-DNP IgG2a (clone Hy1.2) and challenged
76 16h later with 200µg TNP(21-31)-BSA i.v. Alternatively, mice were injected with 1mg of heat-
77 aggregated (1 hour at 63°C in BBS pH8) human IVIG; considering that mouse FcγRI cross-binds
78 human IgG subclasses 1, 3 and 4 [27]. Central temperature was monitored using a digital
79 thermometer with rectal probe (YSI).

80

81 **2.5 Experimental Thrombocytopenia**

82 Blood samples were taken in EDTA before and at indicated time points after i.v. injection of 3 or
83 10µg anti-platelet mAb 6A6. Some mice were treated 32h before 6A6 injection with 300µL PBS-
84 or clodronate- liposomes i.v. Platelet counts were determined using an ABC Vet automatic blood
85 analyser (Horiba ABX).

86

87 **2.6 Tumour Immunotherapy**

88 Mice were depilated and received 5×10^5 B16-Luc2+ cells s.c. on d0. Where indicated, mice were
89 injected i.v. with 200µg mAb TA99 on d1, d2 and d3 (Figure 4A, closed symbols), and control
90 groups were untreated (Figure 4A, open symbols). Bioluminescence was acquired from
91 anaesthetised mice on d1, d7 and d13, 10 min after injection of 75µg luciferin s.c. (IVIS
92 Spectrum CT, Caliper Life Sciences), and images were analysed with Living Image software.

93

94 **2.7 Anti-mouse CD20 treatment**

95 Mice received a single i.v. injection of 50µg anti-mouse CD20 (clone 5D2, IgG2a, Genentech) to
96 deplete endogenous B cells, or saline control, and CD19⁺B220⁺ B cells in the blood, spleen and

97 inguinal lymph nodes were assessed 16 hours later by flow cytometry. Remaining B cells were
98 calculated as a percentage of the average of vehicle-treated controls (Fig. 4B).

99

100 **2.7 Statistics**

101 Data was analysed using one-way ANOVA with Bonferroni post-test (Fig.2C) or a Tukey's
102 multiple comparisons test (Fig.1 B) to compare individual timepoints (Fig.2 B, D & E, and Fig.3
103 A, B & E), or a Kruskal-Wallis test with Dunn's multiple comparisons (Fig. 2A & 2C, bottom
104 panel); a Student's t-test (Fig.3 C&D, Fig.4B) or a Mann-Whitney test (Fig.4A). Statistical
105 significance is indicated (ns: $p>0.05$; * $p<0.05$; ** $p<0.01$, *** $p<0.001$, **** $p<0.0001$).

106

107 **Please refer to supplemental Methods** for information on reagents, flow cytometry, histology,
108 surgical procedures and Active Systemic Anaphylaxis (ASA).

109

3. RESULTS & DISCUSSION

110

111

112

113

114

115

116

117

118

119

120

121

122

123

124

125

126

127

128

129

130

131

132

133

To evaluate the *in vivo* effector functions of mouse FcγRI, we investigated mice expressing this receptor in the absence of other endogenous classical FcγR (FcγRIIB, FcγRIII and FcγRIV-deficient), termed FcγRI^{only} mice [17] or VG1505 mice [28], in comparison with mice deficient for all four endogenous classical FcγRs (FcγRI, FcγRIIB, FcγRIII and FcγRIV-deficient), termed FcγR^{null} mice (Fig.1A). Both strains retain FcRn and non-classical IgG receptor expression. FcγRI^{only} and FcγR^{null} mice display normal breeding patterns and development, and no overt pathological signs up until 1 year of age. We assessed the circulating immune cell populations in these novel strains, compared to WT mice, using an automated blood cell analyser (Fig.1B). Across a large sample size, WT, FcγRI^{only} and FcγR^{null} mice display comparable total leukocyte counts in the blood, and similar frequencies of leukocytes, granulocytes and eosinophils (Fig.1B). Notably, FcγRI^{only} and FcγR^{null} mice have a slightly higher frequency of circulating monocytes. The pattern of expression of FcγRI in FcγRI^{only} mice was comparable to wt mice: FcγRI was detected on circulating Ly6C^{hi} and Ly6C^{low} monocytes (Fig.1D), with greater expression on the latter, and on CD11b⁺CD11c⁺ spleen cells, liver kupffer cells and liver macrophages, alveolar macrophages and bone marrow monocytes (not shown) and prominently on CD11b⁺ skin resident cells (Fig.1E), but barely detected on F4/80⁺ peritoneal macrophages, in agreement with previous reports [24, 29, 30].

An understanding of the participation of FcγRI in autoimmune and inflammatory pathologies remains elusive [4]. FcγRI^{-/-} mice seem to experience reduced inflammation associated with immune complex tissue deposition [13] and severity of antigen-induced arthritis [11, 12]. Yet redundancy between FcγRI and FcγRIII certainly exists [12] and many of these

134 earlier studies did not consider the potential contribution of FcγRIV [14, 24]. To address whether
135 FcγRI can play an effector role in inflammatory autoimmunity, we subjected FcγRI^{only} and
136 FcγR^{null} mice to the K/BxN passive serum transfer model of autoimmune rheumatoid arthritis
137 (K/BxN PA) [31]. Transfer of K/BxN serum into wt mice induced inflammatory signs of arthritis,
138 and an arthritic score which peaked at day 4-6 and remained elevated until day 10 following
139 serum transfer (Fig.2A&B), yet the same volume transferred into FcγRI^{only} or FcγR^{null} mice did
140 not induce arthritis. Histological assessment of ankle joints confirmed marked to severe arthritis
141 in wt mice, and no microscopic signs of arthritis observed in either FcγRI^{only} or FcγR^{null} mice
142 (Supplementary Fig.1A-F). Moreover, K/BxN serum transfer at a dose higher than which was
143 sufficient to induce arthritis in FcγRIV^{only} mice [24] did not result in arthritis induction in
144 FcγRI^{only} mice (Supplementary Fig.1G), indicating that FcγRI alone cannot induce significant
145 cellular infiltration and inflammation associated with this K/BxN model of autoimmune
146 rheumatoid arthritis.

147 During experimental antigen-induced arthritis (EAIA), FcγRI^{-/-} mice were reported to
148 experience comparable joint swelling but a reduction in severe cartilage destruction compared to
149 wt mice [11, 12]. Importantly, EAIA relies first on antigen uptake and presentation, a known
150 functionality of FcγRI [13] on monocyte-derived dendritic cells, leading to the activation of
151 antigen-specific T and B cells and to pathogenic antibody production, and thereafter to FcγR-
152 mediated effector functions. Antigen uptake and presentation is not required in the K/BxN
153 passive arthritis model, as pathogenic antibodies are directly injected into the recipient mouse.
154 Because the severity of K/BxN passive arthritis is not affected in FcγRI^{-/-} mice [25], and because
155 FcγRI^{only} mice are resistant to this arthritis model (this report), FcγRI evidently does not induce
156 the required effector functions to engender arthritic symptoms after K/BxN serum transfer. If this
157 inability extends also to the EAIA model, one may propose that the reduced severity of EAIA

158 observed in FcγRI^{-/-} mice is attributable rather to reduced antigen uptake and presentation.
159 Furthermore, the cardinal marker of cartilage destruction used in EAIA studies relies on the
160 release of matrix metalloproteinases (MMPs) and the creation of neo-epitopes [11, 32]. Therefore
161 although FcγRI does not mediate cell recruitment and joint inflammation in either of these
162 arthritis models (Fig.2A and [11, 12]), it may contribute to reaction severity via local events in
163 the tissue, *i.e.* MMP release and cartilage destruction.

164
165 The K/BxN model of autoimmune rheumatoid arthritis relies on local generation of IgG-
166 immune complexes on the cartilage surface, that trigger the activation of FcγR-expressing cells.
167 To determine if FcγRI can induce local inflammation in another context, we induced IgG-
168 immune complexes at another anatomical site, the airways, and examined the resulting alveolitis.
169 The inflammatory response in wt mice is characterised in the bronchoalveolar lavage (BAL) by
170 massive neutrophil infiltration, significant infiltration of Ly-6C⁺ monocytes, and damage to the
171 airways with haemorrhage into the BAL 16h after challenge (Fig.2C) [26]. Neither FcγR^{null} mice
172 nor FcγRI^{only} mice experienced significant local inflammation: only a mild neutrophil infiltration
173 was observed in the absence of inflammatory monocytes and haemorrhage. Together, our data
174 support the notion that FcγRI does not mediate significant immune cell recruitment and
175 inflammation associated with IgG-immune complex deposition, but may contribute to reaction
176 severity via local events in the tissue, as suggested by studies using FcγRI^{-/-} mice [13, 14].

177
178 Local inflammatory reactions, such as that which drive autoimmune arthritis, require the
179 activation of several cell populations including monocytes/macrophages and neutrophils.
180 Systemic inflammatory reactions like severe hypersensitivity reactions, or anaphylaxis, can also
181 proceed through pathways dependent on IgG and IgG receptors, yet symptoms may arise

182 following the activation of only one cell population, among monocyte/macrophages, neutrophils
183 and basophils (reviewed in [5, 33]). Fc γ RI may participate in such reactions by its expression on
184 monocyte/macrophages. Although Fc γ RI^{-/-} mice were reported to experience mouse IgG2a-
185 induced passive systemic anaphylaxis (PSA) with reduced severity [11], we could not reproduce
186 these findings [34]. Here we demonstrate that Fc γ RI^{only}, like Fc γ R^{null} mice, were resistant to
187 mouse IgG2a-mediated anaphylaxis (Fig.2D), heat-aggregated human IVIG-mediated
188 anaphylaxis (Fig.2E) and even to an active model of anaphylaxis induced by BSA immunization
189 and challenge (Supplementary Fig.3). Two possibilities emerge from these findings: firstly, that
190 Fc γ RI alone is incapable of triggering sufficient inflammatory mediator release to cause systemic
191 symptoms; secondly, that Fc γ RI expression is insufficient when expressed only on
192 monocyte/macrophages to mediate anaphylaxis induction.

193

194 Since we found that Fc γ RI is not sufficient to mediate IgG-induced local or systemic
195 inflammation that require cell recruitment and activation, and release of mediators, we wondered
196 if Fc γ RI was able to induce IgG-mediated cell depletion through phagocytosis and/or ADCC
197 mechanisms that contribute to several autoimmune diseases (*e.g.* autoimmune thrombocytopenia
198 and anaemia) and to immunotherapies. Earlier studies using Fc γ RI^{-/-} mice indicated that Fc γ RI
199 contributes to experimental autoimmune haemolytic anaemia induced by RBC-targeting mIgG2a
200 antibodies [11], particularly to more severe manifestations at high Ab doses [35]. To determine if
201 Fc γ RI has autoimmune destructive properties in Fc γ RI^{only} mice, we examined another model of
202 autoimmunity characterised by circulating immune complexes, immune thrombocytopenic
203 purpura (ITP) induced by injecting anti-platelet antibodies intravenously. ITP could be induced in
204 wt and Fc γ RI^{only} mice, but not Fc γ R^{null} mice (Fig.3A). Within 4 hours of mAb injection,
205 circulating platelet levels were reduced to <20% of their initial concentration in both wt and

206 Fc γ RI^{only} mice (Fig.3A&B), and platelet counts remained low even 24 hours later. Administration
207 of platelet-targeting mAb at a threefold-reduced dose was also sufficient to induce platelet
208 clearance in Fc γ RI^{only} mice, comparable to that of WT mice (Supplementary Fig.4A&B). High-
209 dose toxic clodronate-containing liposomes, administered i.v. to deplete monocyte/macrophages
210 mainly in the blood, spleen, and liver, protected against ITP induction in both WT and Fc γ RI^{only}
211 mice (Fig.3C), indicating that monocytes and macrophages are responsible for platelet clearance.
212

213 To investigate the organ-specific macrophage population responsible for Fc γ RI-dependent
214 autoimmune platelet clearance, we subjected Fc γ RI^{only} mice to either removal of the spleen
215 (splenectomy), or partial removal of the liver (hemi-hepatectomy), prior to ITP induction (Figure
216 3D&E). ITP induction in Fc γ RI^{only} mice was mildly inhibited by splenectomy (Figure 3D):
217 comprising an average reduction in platelet clearance from 88% (\pm 4.2%) to 77% (\pm 9%) 3.5 hours
218 after mAb injection. Splenectomised Fc γ RI^{only} and WT mice had somewhat elevated platelet
219 counts at baseline, whether sampled 1 week or 3 weeks post-surgery, yet notably spleen removal
220 did not inhibit ITP induction in WT mice (Supplementary Fig 4C, and data not shown). These
221 findings suggest that splenic macrophages have a minor contribution to Fc γ RI-dependent ITP.
222 Conversely, partial removal of the liver, which amounted to about 50% reduction in liver mass
223 [36], did not affect ITP induction in Fc γ RI^{only} mice (Figure 3E and Supplementary Fig 4F),
224 suggesting that liver macrophages may not be mandatory for Fc γ RI-dependent ITP. We
225 performed ITP experiments starting 4-5 days after hepatectomies or sham surgeries, due to the
226 rapid regenerative potential of the liver. Importantly, despite the inflammatory effect of the
227 surgical procedures, we did not see differences in Fc γ RI expression on circulating cells between
228 sham operated and hemi-hepatectomised mice (data not shown). It is difficult to completely
229 exclude a role for the liver in this model, as the part of the organ remaining after hemi-

230 hepatectomy may be sufficient to efficiently mediate ITP. Moreover, considerable platelet
231 clearance was still observed in splenectomised mice, which implies the involvement of another
232 physiological site; potentially blood monocytes [37]. Collectively, our data indicate a minor
233 contribution of splenic macrophages to FcγRI-dependent ITP, but do not provide evidence of a
234 role for liver macrophages.

235

236 Antibody-mediated therapies are now a frontline treatment for many malignancies,
237 including a number of autoimmune diseases. Reports using FcγRI^{-/-} mice suggest that FcγRI
238 contributes to IgG-induced tumour cell depletion in the lung [15] and liver [16] but not the skin
239 [20]. As the latter finding may be due to redundant functions among mouse FcγRs in the skin, we
240 followed TYRP-1⁺ Luc2⁺ B16 melanoma cells tumour growth by bioluminescent imaging *in vivo*
241 [17] in mice treated or not with anti-TYRP-1 mouse IgG2a TA99 mAb. Identical growth kinetics
242 were detected in FcγRI^{only} and FcγR^{null} mice (Fig.2F; WT mice in Supplementary Fig.5A), and
243 repeated TA99 injections dramatically reduced tumour load in FcγRI^{only} mice, but not in FcγR^{null}
244 mice, to that of background levels (Fig.4A and Supplementary Fig.5). Thus FcγRI^{only} mice reveal
245 FcγRI-mediated functions that can remain masked in FcγRI^{-/-} mice. Furthermore, these data
246 reinforce the previously reported anti-tumour effector function of FcγRI in lung and liver tissues
247 [15-18] and extends it to the skin tissue.

248

249 Anti-CD20 therapy to deplete B cells has been highly successful in the treatment of B cell
250 malignancies and autoimmune disorders. B cell depletion is known to depend on FcR-dependent
251 mechanisms [38], primarily phagocytosis by Kupffer cells in the liver [36]. A role for FcγRI in
252 the clearance of both malignant and endogenous B cells, in cooperation with FcγRIII and
253 FcγRIV, has been suggested by several studies [18, 39], but has not been formally demonstrated.

254 Since FcγRI was sufficient to mediate destructive platelet clearance (Fig.3), and is expressed on
255 liver Kupffer cells, we tested the capacity of FcγRI to deplete endogenous B cells in a model of
256 anti-CD20 therapy. Administration of mouse CD20-targeting mAb 5D2 (IgG2a) induced B cell
257 depletion in the blood, spleen and lymph nodes of FcγRI^{only}, but not FcγR^{null} mice. 16 hours after
258 treatment 85% of B cells were cleared from the blood and 25-30% of B cells from the secondary
259 lymphoid organs of anti-CD20 treated FcγRI^{only} mice. These data demonstrate that FcγRI, in the
260 absence of FcγRIII and FcγRIV, is sufficient to mediate endogenous B cell clearance, and
261 support a contribution for FcγRI to the efficacy of anti-CD20 therapy in models of lymphoma
262 and autoimmunity.

263

264 In conclusion, genetically modified FcγRI^{only} mice enabled us to demonstrate that the
265 mouse high-affinity IgG receptor FcγRI is sufficient to mediate IgG-induced autoimmune
266 thrombocytopenia and IgG-based immunotherapy targeting either B cells (anti-CD20) or
267 subcutaneous melanoma, in the absence of FcγRIIB, FcγRIII and FcγRIV. FcγRI alone is,
268 however, insufficient to induce IgG-induced autoimmune rheumatoid arthritis, airway
269 inflammation and systemic anaphylaxis, probably due to its inability to efficiently mediate Ab-
270 induced cell recruitment or release of inflammatory mediators. Rather we identify that FcγRI
271 mediates Ab-induced cell depletion/destruction, in both pathogenic autoimmune and therapeutic
272 anti-tumour contexts; which agrees with the important contributions of this receptor to pathogen
273 elimination [11, 40, 41] and antigen uptake and presentation [13]. Furthermore, our data attribute
274 FcγRI-dependent phagocytic function to macrophages in the skin and the spleen. Finally, the
275 effector capabilities of mouse FcγRI appear aligned with its restricted expression profile: low to
276 moderate expression on monocytes, tissue macrophages and monocyte-derived DCs, who are

277 indeed responsible for clearance of foreign bodies and antigen uptake, whereas that of its human
278 homolog hFcγRI extend to pro-inflammatory and pro-anaphylactic functions attributable to more
279 promiscuous expression, particularly high on circulating monocytes and neutrophils. In
280 conclusion, mice models expressing only one particular IgG receptor, *e.g.* FcγRI^{only} or FcγRIV^{only}
281 mice [17, 22-24], are particularly useful to ascribe independent functions to FcγRs, as distinct
282 from potential cooperative roles with other FcγR, the latter of which may be implied from studies
283 using specific FcγR^{-/-} mice.

284

285

4. ACKNOWLEDGMENTS

286
287 We are thankful to O. Godon, B. Iannascoli, B. Todorova and O. Richard-LeGoff for
288 technical help; the members of the Unit of Dynamics of Immune Responses for experimental
289 advice and discussion; the Service Communication Institutionnelle et Image, Institut Pasteur,
290 Paris, for photography work (Supplementary Figure 3D); A-M. Nicola (Plate-Forme d'Imagerie
291 Dynamique, Institut Pasteur, Paris) for help with bioluminescence experiments; and D. Sinnaya
292 for administrative help (Institut Pasteur, Paris). We are thankful to our colleagues for their
293 generous gifts: D. Mathis and C. Benoist (HMS, Boston, MA, USA) and IGBMC (Illkirch,
294 France) for K/BxN mice, R. Good (USFCM, Tampa, FL, USA) for IgG2a mAb 6A6, S. Izui
295 (University of Geneva, Geneva, Switzerland) for IgG2a mAb Hy1.2, Genentech for anti-mouse
296 CD20 mAb 5D2, and N. Van Rooijen (VU Medical Center, The Netherlands) and Roche
297 Diagnostics GmbH for liposomes and Cl2MDP, respectively. This work was mainly supported by
298 the Institut Pasteur and the Institut National de la Santé et de la Recherche Médicale (INSERM);
299 anaphylaxis studies were specifically supported by funding from the European Research Council
300 (ERC)–Seventh Frame-work Program (ERC-2013-CoG 616050). C.G. was supported partly by a
301 stipend from the Pasteur - Paris University (PPU) International PhD program and by the Institut
302 Carnot Pasteur *Maladies Infectieuses*, and partly by the Balsan company. P.P.Z. was supported
303 by FAPESP, process number 2014/233533-9. F.J. is an employee of the Centre National de La
304 Recherche Scientifique (CNRS). H.B. is supported by a fellowship from the University Pierre et
305 Marie Curie.

5. CONFLICT OF INTEREST STATEMENT

307 L.E.M and A.M. are employees of Regeneron Pharmaceuticals, Inc. and hold stock in the
308 company. C.G., H.B., F.J., L.F., S.C., D.A.M., P.P.Z., P.Bouso and P.Bruhns declare no
309 competing financial interests.

6. REFERENCES

- 311 [1] Bruhns P. Properties of mouse and human IgG receptors and their contribution to disease
312 models. *Blood*, 2012;119:5640-9.
- 313 [2] Bruhns P, Jonsson F. Mouse and human FcR effector functions. *Immunol Rev*,
314 2015;268:25-51.
- 315 [3] Nimmerjahn F, Ravetch JV. Fcgamma receptors: old friends and new family members.
316 *Immunity*, 2006;24:19-28.
- 317 [4] van der Poel CE, Spaapen RM, van de Winkel JG, Leusen JH. Functional characteristics
318 of the high affinity IgG receptor, FcgammaRI. *J Immunol*, 2011;186:2699-704.
- 319 [5] Gillis C, Gouel-Cheron A, Jonsson F, Bruhns P. Contribution of Human FcgammaRs to
320 Disease with Evidence from Human Polymorphisms and Transgenic Animal Studies.
321 *Frontiers in immunology*, 2014;5:254.
- 322 [6] Bogdanovich S, Kim Y, Mizutani T, Yasuma R, Tudisco L, Cicatiello V *et al*. Human
323 IgG1 antibodies suppress angiogenesis in a target-independent manner. *Signal Transduct*
324 *Target Ther*, 2016;1.
- 325 [7] Bevaart L, Van Ojik HH, Sun AW, Sulahian TH, Leusen JH, Weiner GJ *et al*. CpG
326 oligodeoxynucleotides enhance FcgammaRI-mediated cross presentation by dendritic
327 cells. *Int Immunol*, 2004;16:1091-8.
- 328 [8] Mancardi DA, Albanesi M, Jonsson F, Iannascoli B, Van Rooijen N, Kang X *et al*. The
329 high-affinity human IgG receptor FcgammaRI (CD64) promotes IgG-mediated
330 inflammation, anaphylaxis, and antitumor immunotherapy. *Blood*, 2013;121:1563-73.
- 331 [9] van Vugt MJ, Heijnen AF, Capel PJ, Park SY, Ra C, Saito T *et al*. FcR gamma-chain is
332 essential for both surface expression and function of human Fc gamma RI (CD64) in
333 vivo. *Blood*, 1996;87:3593-9.
- 334 [10] McIntosh RS, Shi J, Jennings RM, Chappel JC, de Koning-Ward TF, Smith T *et al*. The
335 importance of human FcgammaRI in mediating protection to malaria. *PLoS Pathog*,
336 2007;3:e72.
- 337 [11] Ioan-Facsinay A, de Kimpe SJ, Hellwig SM, van Lent PL, Hofhuis FM, van Ojik HH *et*
338 *al*. Fc gamma RI (CD64) contributes substantially to severity of arthritis, hypersensitivity
339 responses, and protection from bacterial infection. *Immunity*, 2002;16:391-402.
- 340 [12] van Lent PL, Nabbe K, Blom AB, Holthuysen AE, Sloetjes A, van de Putte LB *et al*. Role
341 of activatory Fc gamma RI and Fc gamma RIII and inhibitory Fc gamma RII in
342 inflammation and cartilage destruction during experimental antigen-induced arthritis. *Am*
343 *J Pathol*, 2001;159:2309-20.
- 344 [13] Barnes N, Gavin AL, Tan PS, Mottram P, Koentgen F, Hogarth PM. FcgammaRI-
345 deficient mice show multiple alterations to inflammatory and immune responses.
346 *Immunity*, 2002;16:379-89.
- 347 [14] Baumann U, Kohl J, Tschernig T, Schwerter-Strumpf K, Verbeek JS, Schmidt RE *et al*. A
348 codominant role of Fc gamma RI/III and C5aR in the reverse Arthus reaction. *J Immunol*,
349 2000;164:1065-70.
- 350 [15] Bevaart L, Jansen MJ, van Vugt MJ, Verbeek JS, van de Winkel JG, Leusen JH. The
351 high-affinity IgG receptor, FcgammaRI, plays a central role in antibody therapy of
352 experimental melanoma. *Cancer Res*, 2006;66:1261-4.

- 353 [16] Otten MA, van der Bij GJ, Verbeek SJ, Nimmerjahn F, Ravetch JV, Beelen RH *et al.*
354 Experimental antibody therapy of liver metastases reveals functional redundancy between
355 Fc gammaRI and Fc gammaRIV. *J Immunol*, 2008;181:6829-36.
- 356 [17] Albanesi M, Mancardi DA, Macdonald LE, Iannascoli B, Zitvogel L, Murphy AJ *et al.*
357 Cutting Edge: FcgammaRIII (CD16) and FcgammaRI (CD64) Are Responsible for Anti-
358 Glycoprotein 75 Monoclonal Antibody TA99 Therapy for Experimental Metastatic B16
359 Melanoma. *J Immunol*, 2012;189:5513-7.
- 360 [18] Minard-Colin V, Xiu Y, Poe JC, Horikawa M, Magro CM, Hamaguchi Y *et al.*
361 Lymphoma depletion during CD20 immunotherapy in mice is mediated by macrophage
362 FcgammaRI, FcgammaRIII, and FcgammaRIV. *Blood*, 2008;112:1205-13.
- 363 [19] Nimmerjahn F, Bruhns P, Horiuchi K, Ravetch JV. Fc gamma RIV: a novel FcR with
364 distinct IgG subclass specificity. *Immunity*, 2005;23:41-51.
- 365 [20] Nimmerjahn F, Lux A, Albert H, Woigk M, Lehmann C, Dudziak D *et al.* FcgammaRIV
366 deletion reveals its central role for IgG2a and IgG2b activity in vivo. *Proc Natl Acad Sci*
367 *U S A*, 2010;107:19396-401.
- 368 [21] Tipton TR, Mockridge CI, French RR, Tutt AL, Cragg MS, Beers SA. Anti-mouse
369 FcgammaRIV antibody 9E9 also blocks FcgammaRIII in vivo. *Blood*, 2015;126:2643-5.
- 370 [22] Mancardi DA, Iannascoli B, Hoos S, England P, Daeron M, Bruhns P. FcgammaRIV is a
371 mouse IgE receptor that resembles macrophage FcepsilonRI in humans and promotes
372 IgE-induced lung inflammation. *J Clin Invest*, 2008;118:3738-50.
- 373 [23] Jönsson F, Mancardi DA, Kita Y, Karasuyama H, Iannascoli B, Van Rooijen N *et al.*
374 Mouse and human neutrophils induce anaphylaxis. *J Clin Invest*, 2011;121:1484-96.
- 375 [24] Mancardi DA, Jonsson F, Iannascoli B, Khun H, Van Rooijen N, Huerre M *et al.* The
376 murine high-affinity IgG receptor Fc(gamma)RIV is sufficient for autoantibody-induced
377 arthritis. *J Immunol*, 2011;186:1899-903.
- 378 [25] Bruhns P, Samuelsson A, Pollard JW, Ravetch JV. Colony-stimulating factor-1-
379 dependent macrophages are responsible for IVIG protection in antibody-induced
380 autoimmune disease. *Immunity*, 2003;18:573-81.
- 381 [26] Jönsson F, Mancardi DA, Zhao W, Kita Y, Iannascoli B, Khun H *et al.* Human
382 FcgammaRIIA induces anaphylactic and allergic reactions. *Blood*, 2012;119:2533-44.
- 383 [27] Overdijk MB, Verploegen S, Ortiz Buijsse A, Vink T, Leusen JH, Bleeker WK *et al.*
384 Crosstalk between Human IgG Isotypes and Murine Effector Cells. *J Immunol*,
385 2012;189:3430-8.
- 386 [28] Gillis CM, Jönsson F, Mancardi DA, Tu N, Beutier H, Van Rooijen N *et al.* Mechanisms
387 of anaphylaxis in human low-affinity IgG receptor locus knock-in mice. *Journal of*
388 *Allergy and Clinical Immunology*, 2016;In press. doi: 10.1016/j.jaci.2016.06.058.
- 389 [29] Tan PS, Gavin AL, Barnes N, Sears DW, Vremec D, Shortman K *et al.* Unique
390 monoclonal antibodies define expression of Fc gamma RI on macrophages and mast cell
391 lines and demonstrate heterogeneity among subcutaneous and other dendritic cells. *J*
392 *Immunol*, 2003;170:2549-56.
- 393 [30] Langlet C, Tamoutounour S, Henri S, Luche H, Ardouin L, Gregoire C *et al.* CD64
394 Expression Distinguishes Monocyte-Derived and Conventional Dendritic Cells and
395 Reveals Their Distinct Role during Intramuscular Immunization. *J Immunol*,
396 2012;188:1751-60.
- 397 [31] Monach PA, Mathis D, Benoist C. The K/BxN arthritis model. *Curr Protoc Immunol*,
398 2008;Chapter 15:Unit 15 22.

- 399 [32] Singer, II, Kawka DW, Bayne EK, Donatelli SA, Weidner JR, Williams HR *et al.*
400 VDIPEN, a metalloproteinase-generated neoepitope, is induced and immunolocalized in
401 articular cartilage during inflammatory arthritis. *J Clin Invest*, 1995;95:2178-86.
- 402 [33] Jonsson F, Mancardi DA, Albanesi M, Bruhns P. Neutrophils in local and systemic
403 antibody-dependent inflammatory and anaphylactic reactions. *Journal of leukocyte*
404 *biology*, 2013;94:643-56.
- 405 [34] Beutier H, Gillis CM, Iannascoli B, Godon M, England P, Sibilano R *et al.* IgG
406 subclasses determine pathways of anaphylaxis in mice. *J Allergy Clin Immunol*, 2016;In
407 press doi: 10.1016/j.jaci.2016.03.028.
- 408 [35] Baudino L, Nimmerjahn F, Azeredo da Silveira S, Martinez-Soria E, Saito T, Carroll M *et*
409 *al.* Differential contribution of three activating IgG Fc receptors (FcγRI, FcγRIII,
410 FcγRIIIb, and FcγRIIIc) to IgG2a- and IgG2b-induced autoimmune hemolytic
411 anemia in mice. *J Immunol*, 2008;180:1948-53.
- 412 [36] Montalvao F, Garcia Z, Celli S, Breart B, Deguine J, Van Rooijen N *et al.* The
413 mechanism of anti-CD20-mediated B cell depletion revealed by intravital imaging. *J Clin*
414 *Invest*, 2013;123:5098-103.
- 415 [37] Biburger M, Aschermann S, Schwab I, Lux A, Albert H, Danzer H *et al.* Monocyte
416 subsets responsible for immunoglobulin G-dependent effector functions in vivo.
417 *Immunity*, 2011;35:932-44.
- 418 [38] Uchida J, Hamaguchi Y, Oliver JA, Ravetch JV, Poe JC, Haas KM *et al.* The innate
419 mononuclear phagocyte network depletes B lymphocytes through Fc receptor-dependent
420 mechanisms during anti-CD20 antibody immunotherapy. *J Exp Med*, 2004;199:1659-69.
- 421 [39] Hamaguchi Y, Xiu Y, Komura K, Nimmerjahn F, Tedder TF. Antibody isotype-specific
422 engagement of Fcγ receptors regulates B lymphocyte depletion during CD20
423 immunotherapy. *J Exp Med*, 2006;203:743-53.
- 424 [40] Mittal R, Sukumaran SK, Selvaraj SK, Wooster DG, Babu MM, Schreiber AD *et al.*
425 Fcγ receptor I alpha chain (CD64) expression in macrophages is critical for the
426 onset of meningitis by *Escherichia coli* K1. *PLoS Pathog*, 2010;6:e1001203.
- 427 [41] Esser-von Bieren J, Volpe B, Kulagin M, Sutherland DB, Guet R, Seitz A *et al.*
428 Antibody-mediated trapping of helminth larvae requires CD11b and Fcγ receptor I.
429 *J Immunol*, 2015;194:1154-63.
- 430

431

432

FIGURE LEGENDS

433

434

435 **Figure 1: FcγRI only mice have normal blood leukocyte composition and show comparable**
436 **FcγRI expression to that of WT mice.** (A) Schematic representation of WT, FcγRI^{only} and
437 FcγR^{null} mice. (B) Leukocyte counts and relative percentages of immune cell populations in the
438 blood of WT (n=20), FcγRI^{only} (n=35) and FcγR^{null} (n=24) mice were enumerated using an
439 automatic blood cell analyser. (C) Representative flow cytometry profiles of FcγRI expression on
440 indicated cell populations from the blood and organs of WT, FcγRI^{only} and FcγR^{null} mice (MΦ;
441 macrophages). Shaded histograms indicate background staining of a mIgG1 isotype control.
442 Staining is representative of at least 2 independent experiments, n≥2.

443

444 **Figure 2: FcγRI alone is insufficient to mediate IgG-induced arthritis, airway inflammation**
445 **or systemic anaphylaxis,** (A-B) Arthritis was evaluated by clinical score (A) and ankle thickness
446 (B) measured following transfer of K/BxN serum (5μL/g body weight) into WT (triangles),
447 FcγRI^{only} (circles) or FcγR^{null} (squares) mice. (A) *p<0.05 on d3-6, WT compared to FcγR^{null}
448 mice; (B) *p<0.05 on d2, **p<0.01 on d3, ***p<0.001 on d4-6, WT compared to FcγR^{null} and
449 FcγRI^{only} mice. Data is representative of >2 independent experiments, n≥3 per group. (C)
450 Bronchoalveolar lavage (BAL) was performed on naive (open symbols, n=3 per group) WT
451 (triangles), FcγRI^{only} (circles) and FcγR^{null} (squares) mice, or mice 16-18h after challenge with
452 antiserum i.n. and OVA antigen i.v. (closed symbols). Neutrophils and Ly6C⁺ macrophages
453 (MΦ) in the BAL were determined by flow cytometry. Haemorrhage was determined by
454 measuring haemoglobin concentration in the BAL supernatant. **p<0.01, *** p<0.001, ****
455 p<0.0001; challenge data is pooled from 2 independent experiments, n=8-10 mice per group. (D-
456 E) Temperature monitoring during passive systemic anaphylaxis (PSA) in WT, FcγR^{null} or

457 FcγRI^{only} mice, induced by (D) mIgG2a anti-TNP sensitization and TNP-BSA i.v. challenge or
458 (E) i.v. injection of aggregated human IVIG. *n*=3-5 per group; data is representative of 2
459 independent experiments. **p*<0.05, ***p*<0.01, **** *p*<0.0001 at all time points from 30min; WT
460 compared to FcγR^{null} and FcγRI^{only} mice.

461

462 **Figure 3: FcγRI-mediated thrombocytopenia is dependent on monocyte/macrophages, and**
463 **partially inhibited by splenectomy.** (A-B) Circulating platelets in the blood of WT (*n*=3),
464 FcγRI^{only} (*n*=7) and FcγR^{null} (*n*=7) mice were quantified at baseline and following i.v. injection of
465 10μg anti-platelet mAb (clone 6A6) and are represented as (A) percentage over time and (B)
466 number of platelets 4 hours after mAb injection; **** *p*<0.0001 at 4h, 9h and 24h, WT vs
467 FcγR^{null} and FcγRI^{only} vs FcγR^{null}. (C) Platelet counts at baseline and 4 hours after mAb injection
468 in mice pre-treated with PBS- (open symbols) or toxic- (closed symbols) liposomes; *n*=4-5 per
469 group; * *p*<0.05, **** *p*<0.0001, significance values indicated for each group at 4 hours
470 compared to baseline. (D-E) ITP induction and percentage of circulating platelets in (D) FcγRI^{only}
471 mice following splenectomy (closed symbols, *n*=11) compared to controls (open symbols, *n*=10);
472 and (E) FcγR^{null} mice (*n*=4) or FcγRI^{only} mice following hemi-hepatectomy (*n*=5), compared to
473 sham operated (*n*=4), or controls (*n*=3); ** *p*<0.01, splenectomised mice compared to controls;
474 **** *p*<0.0001 at 3.5h, 8h and 24h, all groups compared to FcγR^{null}; ns not significant. Data in
475 (D&E) is pooled from two independent experiments.

476

477 **Figure 4: FcγRI is sufficient for anti-melanoma and B cell depletion therapies.**
478 (A) FcγRI^{only} (circles) or FcγR^{null} (squares) mice were injected with B16-Luc2⁺ cells s.c. on d0
479 and received no treatment (open symbols) or mAb TA99 i.v. on day 1, 2 and 3 (closed symbols);
480 tumour growth was monitored by bioluminescent signal after s.c. injection of luciferin.

481 **(B)** FcγRI^{only} (circles) or FcγR^{null} (squares) mice were injected with anti-CD20 mAb 5D2 (closed
482 symbols) or vehicle (open symbols). The percentage of remaining CD19⁺B220⁺ B cells
483 (compared to the average of vehicle-treated controls) was determined in the blood, spleen and
484 inguinal lymph nodes after 16h later. Data in **(A)** is representative of 2 independent experiments,
485 $n=4-5$ per group. Data in **(B)** is pooled from 2 independent experiments, $n=3-5$ per group.
486 * $p<0.05$ on day 7 and day 13, *** $p<0.001$, **** $p<0.0001$, FcγRI^{only} controls compared to mAb-
487 treated; ns not significant, FcγR^{null} controls compared to mAb-treated.
488

Supplemental Materials and Methods

Reagents

Human IVIG (Gamunex®) was from Grifols, containing 63% hIgG1, 29% hIgG2, 5% hIgG3 and 3% hIgG4. B16-Luc2+ cells were from Caliper-Life Sciences. IgG were purified by Protein G-affinity purification from supernatants of hybridomas producing anti-gp75 mAb (TA99) from American Type Culture Collection, mIgG2a anti-platelet mAb (clone 6A6) provided by Dr R. Good (USFCM, Tampa, FL, USA), and mIgG2a anti-TNP mAb (Hy1.2) provided by Shozo Izui (University of Geneva, Geneva, Switzerland). Luciferin was from Invitrogen, rabbit anti-OVA antiserum, OVA, BSA, and Freund's adjuvant (CFA/IFA) were from Sigma-Aldrich, TNP₍₂₁₋₃₁₎-BSA was from Santa Cruz and PBS- and clodronate-liposomes were prepared as previously described [1]. Vivotag-680 was from Perkin Elmer and OVA-vivotag-680 was prepared as recommended by the manufacturer.

Tissue processing and flow cytometry

Spleens were dissociated through a 70µm cell strainer into MACS buffer (PBS /0.5%BSA /2mM EDTA) and RBC lysis was performed using an ammonium chloride-based buffer. For isolation of skin cells, ears were split into dorsal and ventral halves and roughly chopped before digestion with 0.25mg/mL Liberase TL ResearchGrade (Roche) + 0.1mg/mL DNase (Sigma) for 1h at 37°C (800rpm; Eppendorf Thermomixer), washed with 10x volume of PBS/ 10%FBS /2mM EDTA and processed through a 100µm cell strainer. Livers were perfused with cold PBS before dissection, and liver leukocytes were isolated using the Liver Dissociation Kit and gentleMACS Octo Dissociator from Miltenyi, according to the manufacturer's

instructions. Cells were isolated from the peritoneum by lavage with 6mL cold PBS; BALs were performed 3x with 1mL PBS. For blood leukocyte analysis, heparinised blood was subjected to RBC lysis with either Red Blood Cell Lysis Solution (Miltenyi) or BD Pharm Lyse Lysing Buffer (BD Biosciences) and washed with MACS buffer. Single cell suspensions were washed with MACS buffer, incubated with 2.4G2 (Fab')₂ fragments (anti-CD16/32, 40µg/mL; 15min on ice) and stained with fluorochrome-conjugated antibodies in MACS buffer for 30min on ice. Data was collected on a MACSQuant flow cytometer (Miltenyi), and analysed using FlowJo Software (TreeStar, Inc.).

Cell populations were defined by FSC/SSC properties and surface markers as indicated (Fig.1B), or in the BAL (Fig.2B): alveolar macrophages (CD11c⁺/ SiglecF⁺), eosinophils (CD11c^{neg}/ SiglecF⁺), neutrophils (CD11c^{neg}/ SiglecF^{neg}/ CD11b⁺/ Ly-6G⁺), Ly-6C⁺ macrophages (CD11c^{neg}/ SiglecF^{neg}/ CD11b⁺/ Ly-6G^{neg}/ Ly-6C⁺).

Active Systemic Anaphylaxis (ASA)

Mice were immunised i.p. on d0 with 200µg BSA in Complete Freund's Adjuvant, and boosted on d14 with 200µg BSA in Incomplete Freund's Adjuvant. BSA-specific IgG1, IgG2a/b/c and IgE serum antibodies were titered by ELISA on d21 as described [2]. Mice with comparable antibody titers were challenged 13-14 days after the last immunisation i.v. with 500µg BSA. Central temperature and mortality was monitored.

Partial hepatectomy and splenectomy

Partial hepatectomy was performed as described[3]. Mice were anaesthetised and a transverse abdominal incision was made. The superior lobes of the liver were laid on the diaphragm and the ligaments of the caudate lobe dissected. The caudate lobe was

then pulled in front of the stomach and resected after in-bloc ligation of its hilum (6/0 silk). The lateral left lobe was resected using the same technique. The abdomen was closed using 4/0 silk running sutures. The procedure removed approximately half of the initial liver mass. Mice were rested for 2 days before experimental procedure. For splenectomy, a small vertical incision was made on the left flank, the spleen was gently pulled outside the abdomen, and the splenic ligaments and vessels were cut. The abdomen was closed with a 4/0 silk suture, and the skin with a surgical staple. Mice were rested for 1-3 weeks before experimental procedure.

Histology

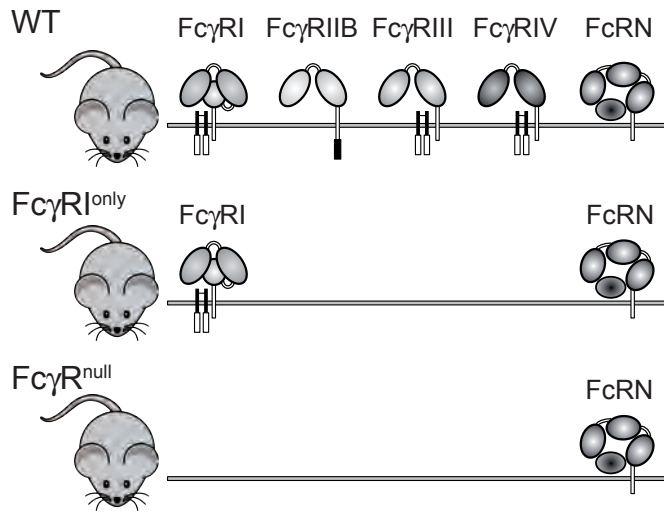
Ankle joints and surrounding tissues (from the extremity of the femur/tibia to the digits) were sampled on day 8 after K/BxN serum transfer (batch #1, 5mL/kg), then fixed and simultaneously decalcified using Formical-4[®] (StatLab Medical Products) for 2 weeks. Samples were routinely embedded in paraffin, and 4 mm sections were stained with haematoxylin and eosin (H&E). Sections were evaluated microscopically and histological changes (*i.e.* inflammation, pannus formation, bone erosion and cartilage damage) were scored from 0 (no change) to 5 (severe).

Supplemental references

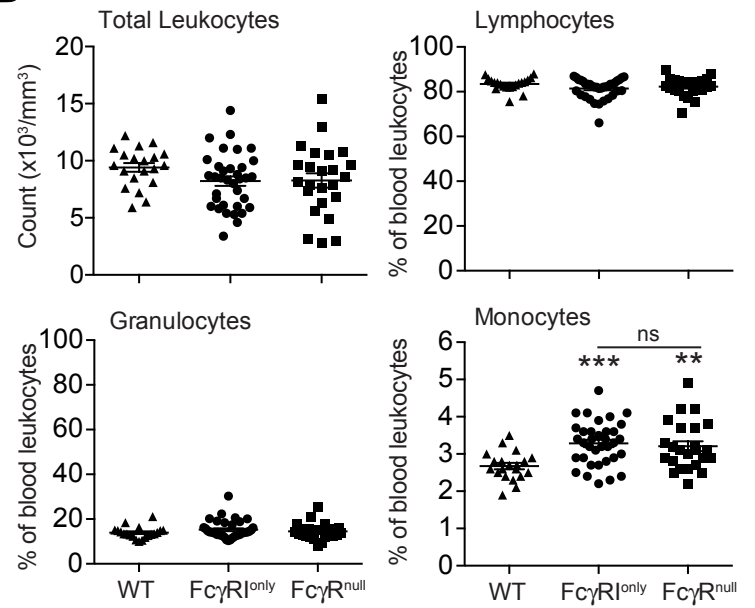
- [1] Van Rooijen N, Sanders A. Liposome mediated depletion of macrophages: mechanism of action, preparation of liposomes and applications. *J Immunol Methods*, 1994;174:83-93.
- [2] Jönsson F, Mancardi DA, Kita Y, Karasuyama H, Iannascoli B, Van Rooijen N *et al.* Mouse and human neutrophils induce anaphylaxis. *J Clin Invest*, 2011;121:1484-96.
- [3] Montalvao F, Garcia Z, Celli S, Breart B, Deguine J, Van Rooijen N *et al.* The mechanism of anti-CD20-mediated B cell depletion revealed by intravital imaging. *J Clin Invest*, 2013;123:5098-103.

Figure 1

A



B



C

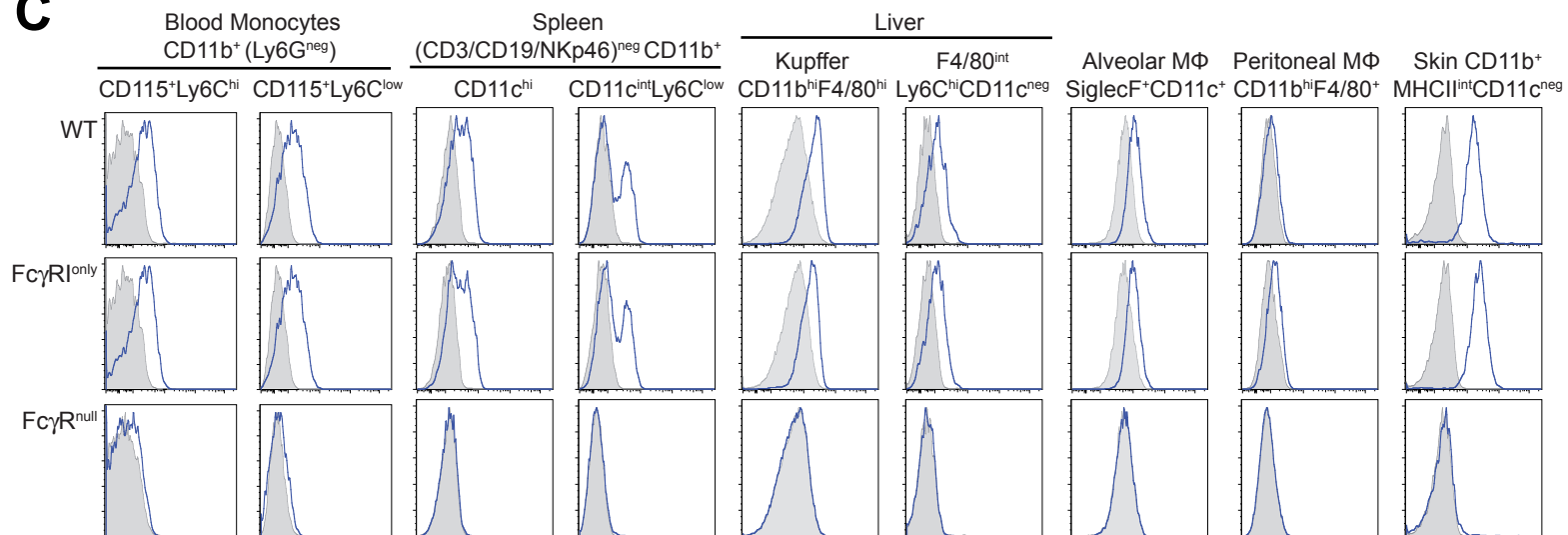


Figure 2

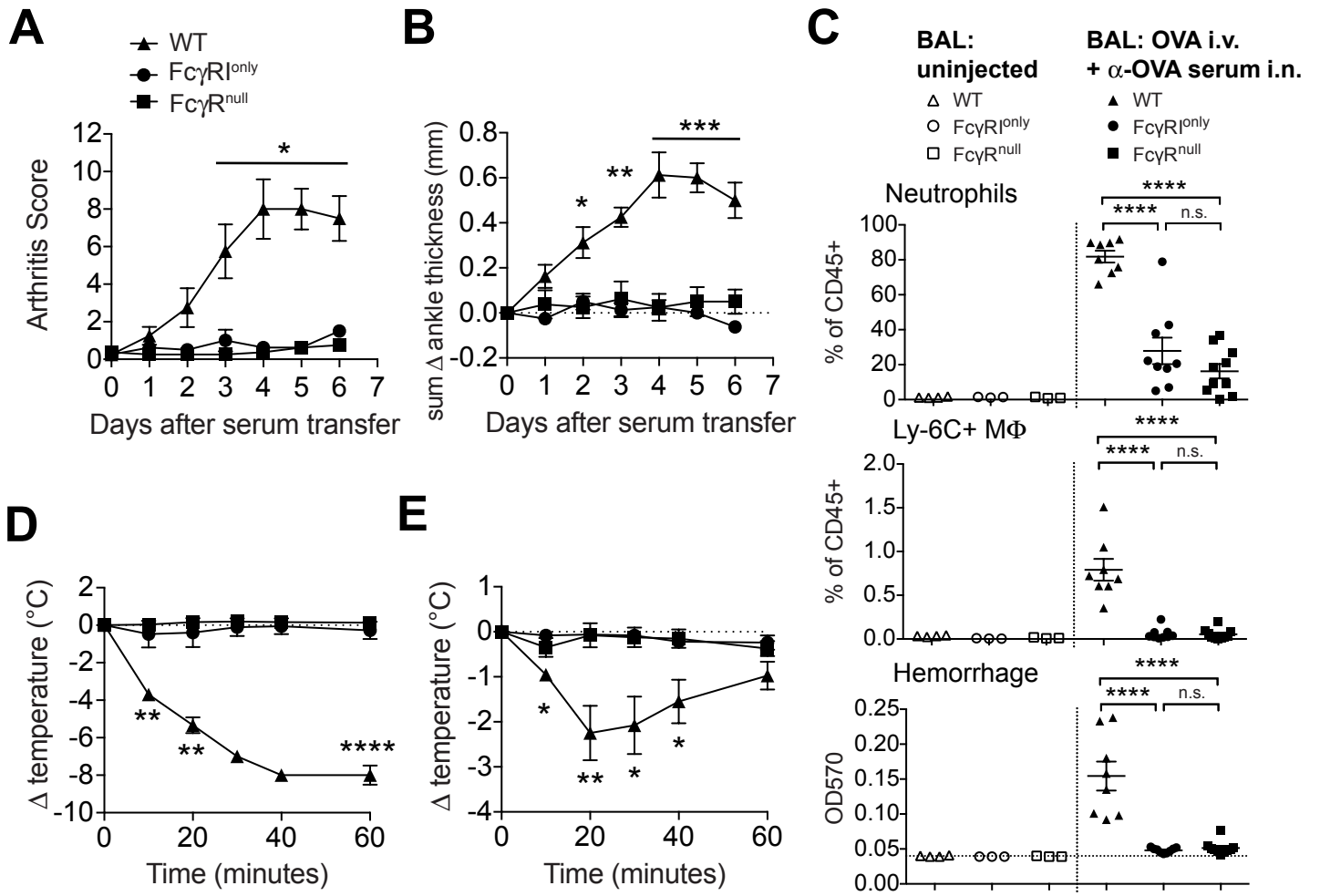


Figure 3

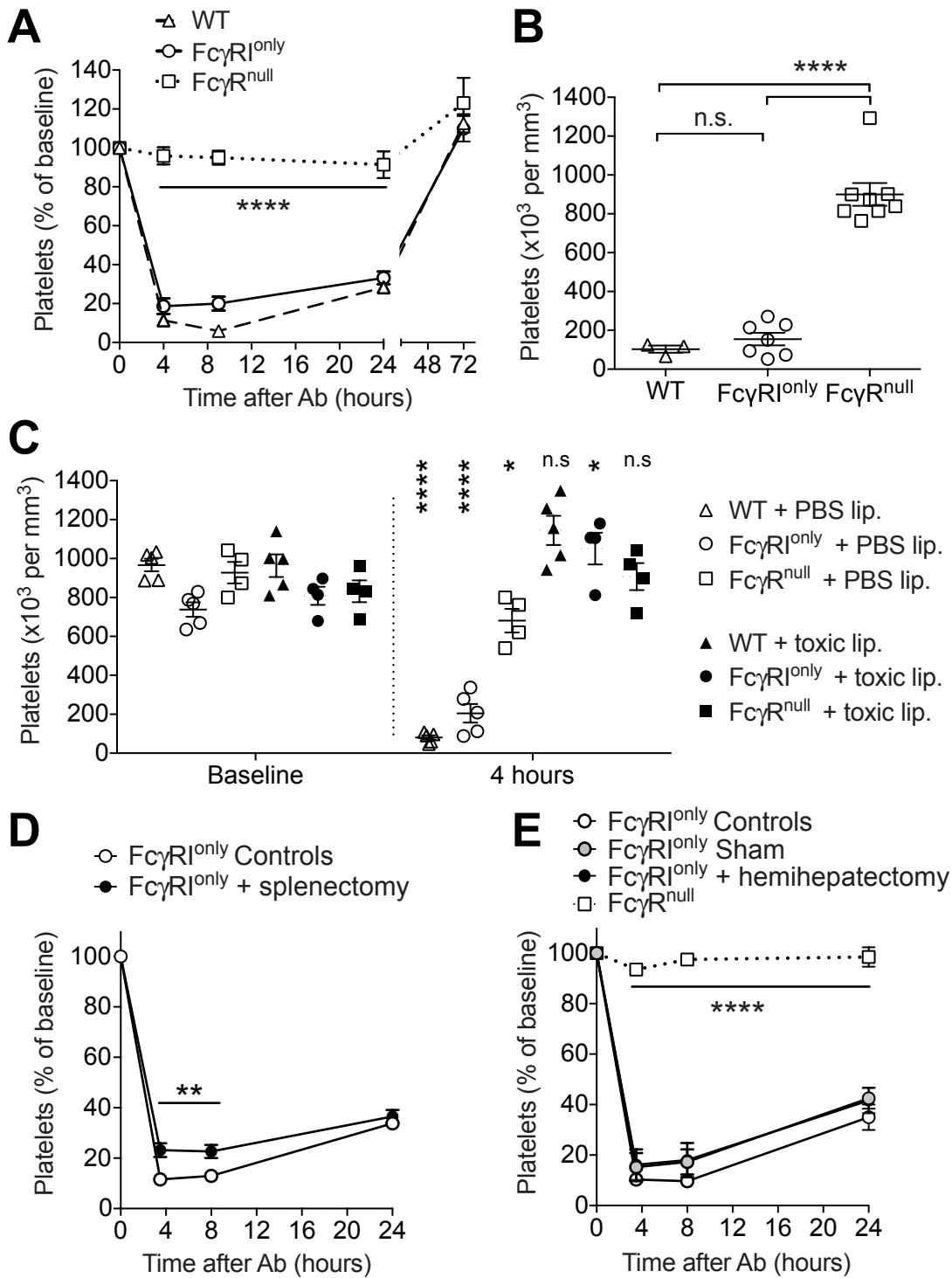
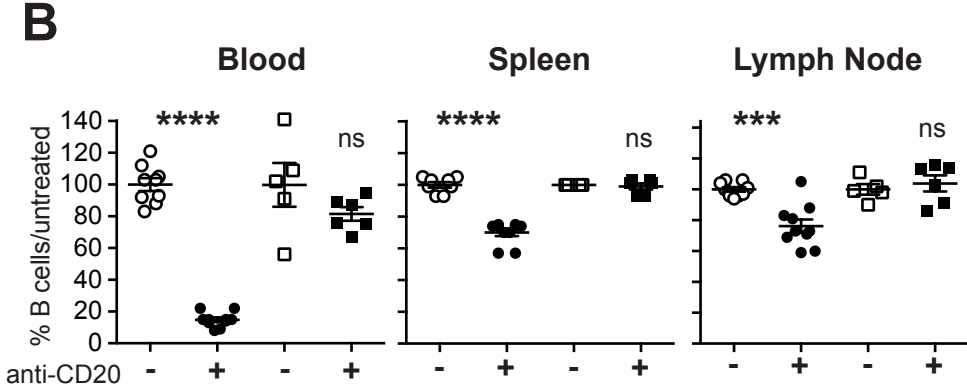
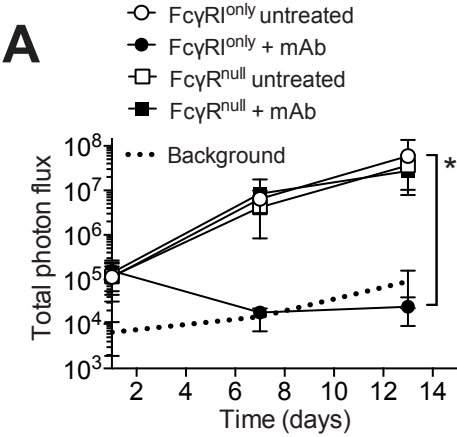
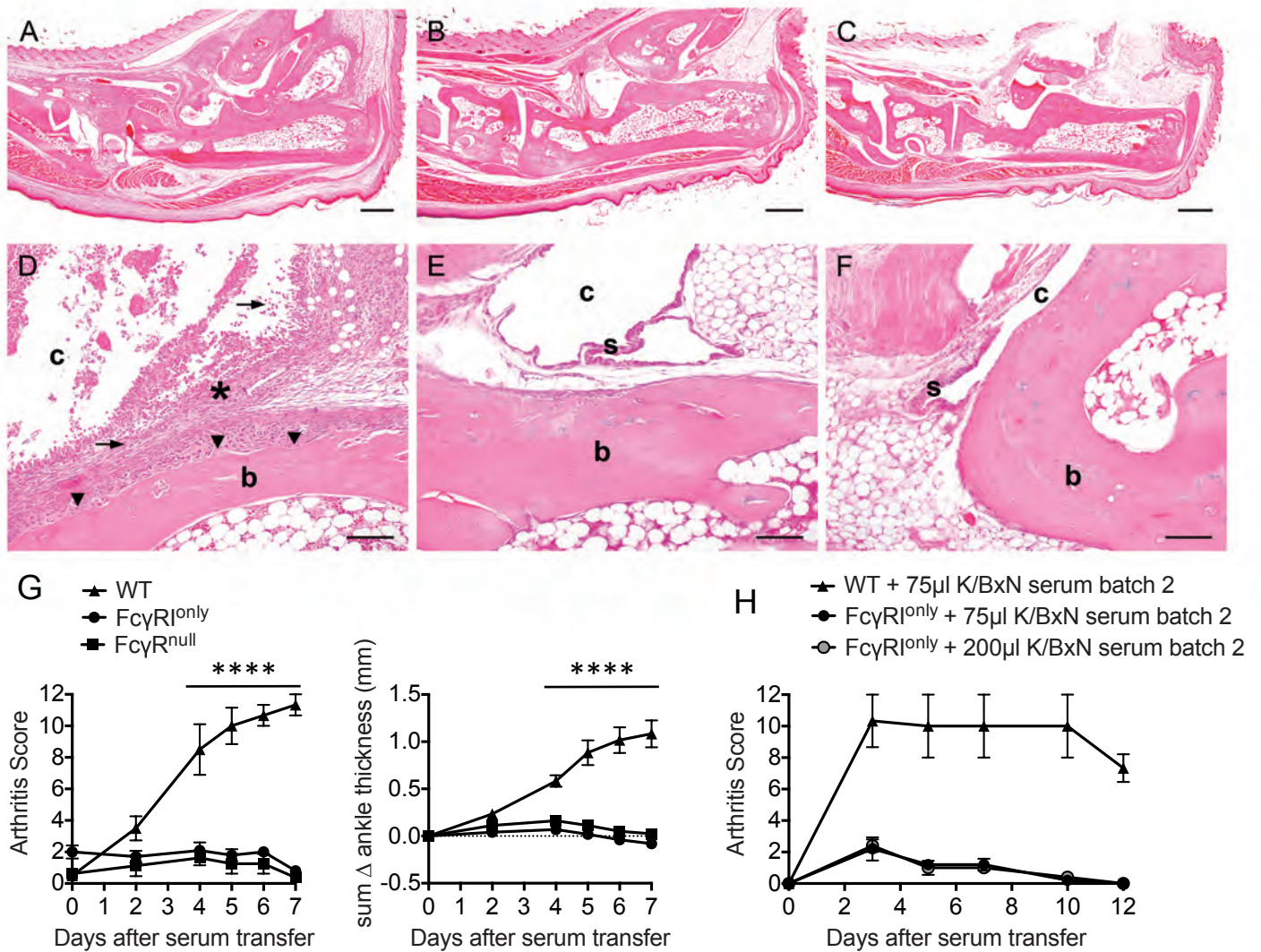


Figure 4

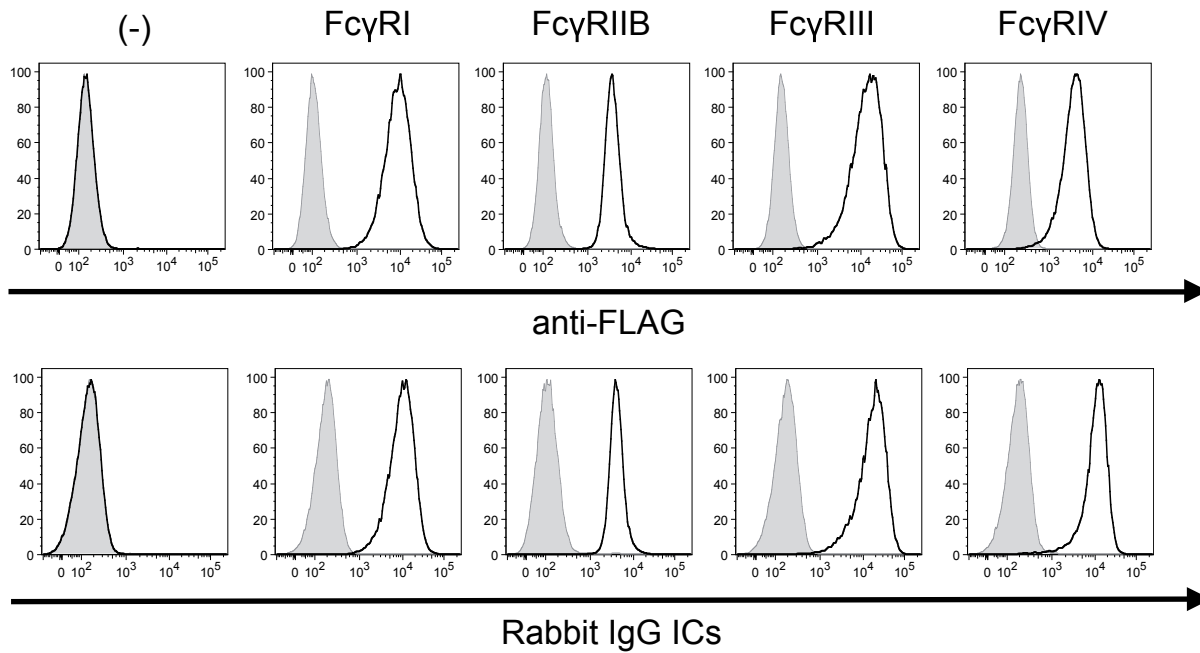


Supplementary Figure 1



Supplementary Figure 1: mFcγRI alone is insufficient to induce arthritis, even with increased dose of administration, or a different batch of K/BxN serum. (A-F) H&E stained paraffin-embedded sections of decalcified ankle joints on day 8 after K/BxN serum transfer (batch #1, 5mL/kg). Histological signs of marked to severe arthritis were noted in WT mice (A, D), and were characterised by neutrophil and mononuclear cell infiltrates (arrow), pannus formation (asterisk), cartilage damage and bone resorption (arrowhead). No microscopic signs of arthritis were observed in FcγR^{null} (B, E) or FcγRI^{only} (C, F) mice. (b: bone; c: synovial cavity, s: synovial membrane). Scale bar: (A, B, C) 500 μm, (D, E, F) 100 μm (G) Arthritic score and ankle thickness following transfer of high-dose K/BxN serum (batch #1, 10mL/kg) into WT (triangles), FcγR^{null} (squares) or FcγRI^{only} (circles) mice, or (H) arthritic score following transfer of K/BxN serum (batch #2, indicated volumes) into WT or FcγRI^{only} mice.

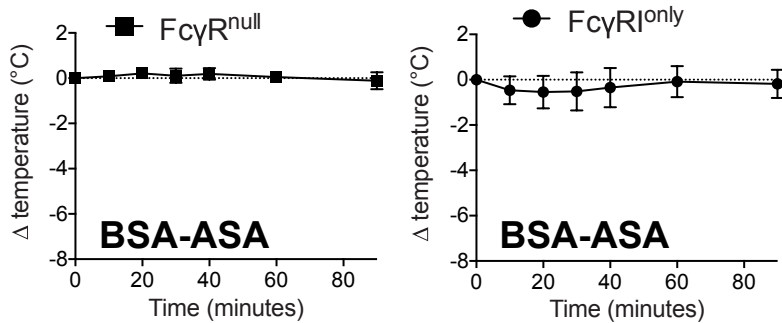
Supplementary Figure 2



Supplemental Figure 2: Fc γ RI binds OVA immune complexes. CHO cells stably transfected to express FLAG-tagged mFc γ RI, mFc γ RIIB, mFc γ RIII, or mFc γ RIV, as indicated, or control cells (-) were stained with an anti-FLAG antibody (upper panel) to confirm receptor expression; shaded histograms represent isotype control staining. CHO transfectants were incubated with immune complexes (ICs) formed by rabbit anti-OVA serum and fluorescently (vivotag680)-tagged OVA (lower panel). Shaded histograms represent background fluorescence (OVA-vivotag680 alone); open histograms IC binding.

Supplementary Figure 3

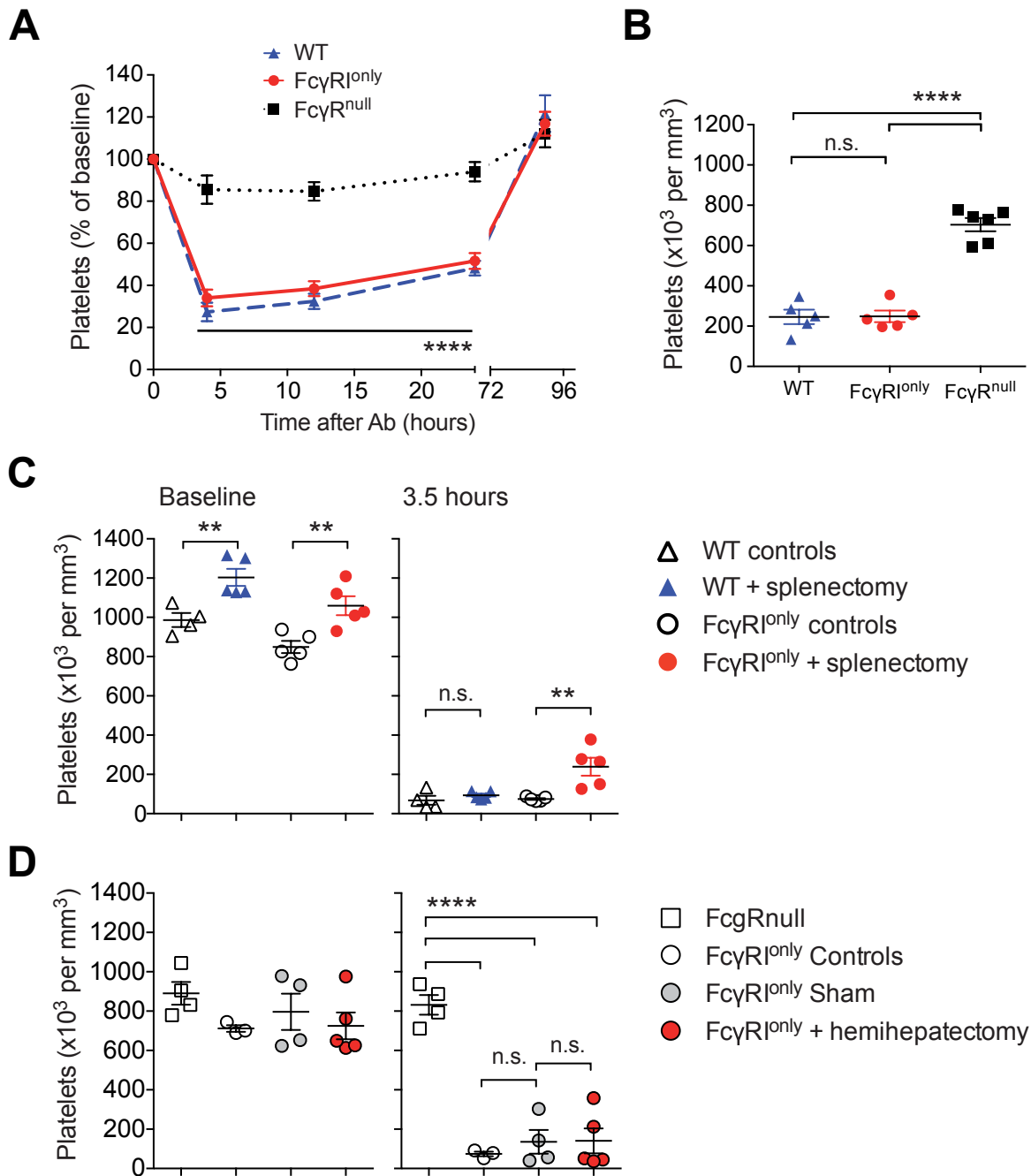
Maximum temp. loss	FcyR ^{null}		FcyR ^{I^{only}}	
	IVIG PSA	BSA ASA	IVIG PSA	BSA ASA
<1°C	56 (100%)	14 (100%)	67 (82,7%)	36 (83,7%)
1-2°C	0	0	6 (7,4%)	5 (11,6%)
>2°C	0	0	8 (9,9%)	2 (4,7%)



Supplementary Figure 3: FcyR^{I^{only}} mice are resistant to BSA-ASA and IVIG-PSA.

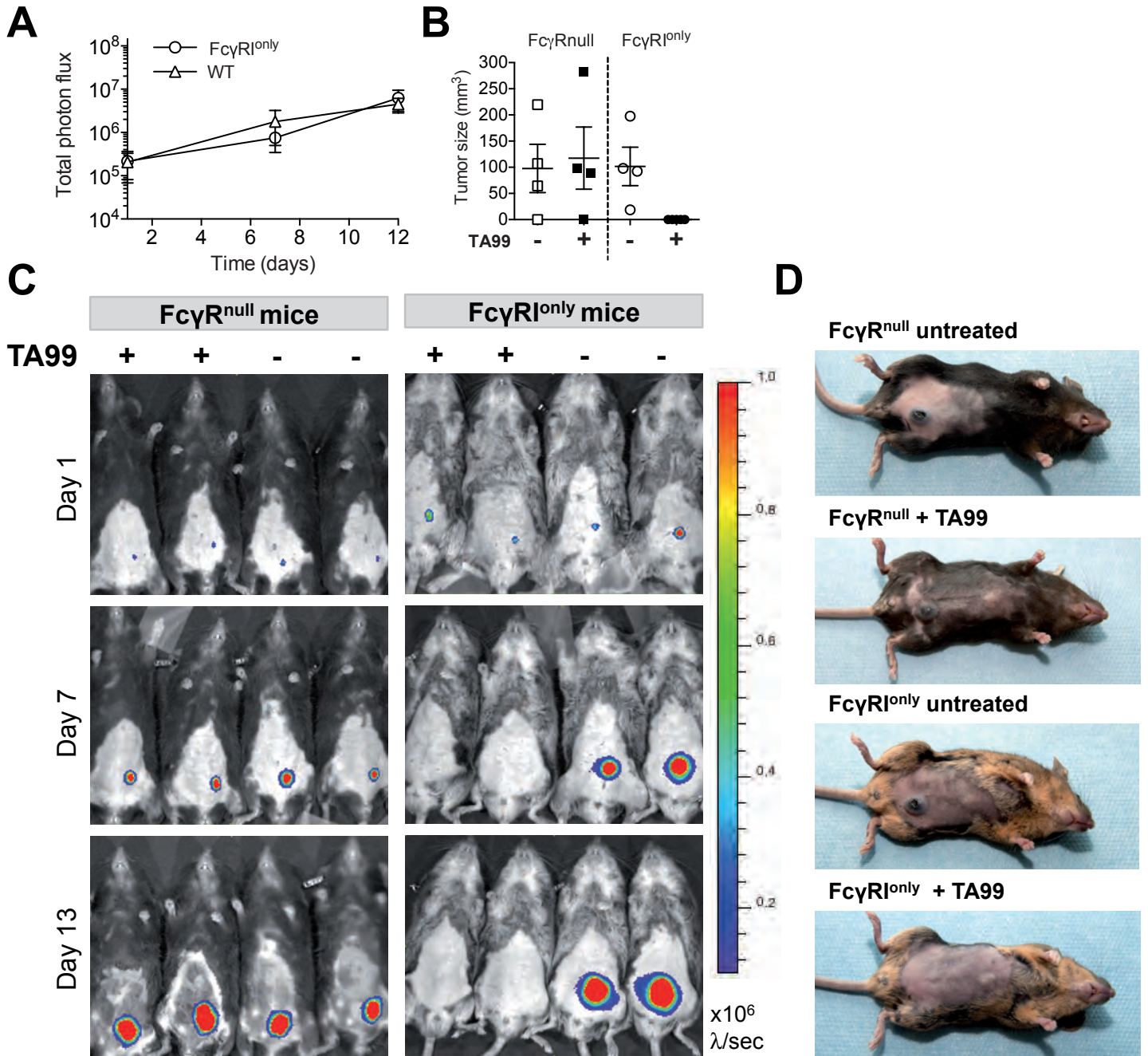
(A) FcyR^{null} (left) and FcyR^{I^{only}} (right) mice were injected with 1mg heat-aggregated IVIG (IVIG-PSA) or immunized and challenged with BSA antigen (BSA-ASA) and central temperatures were monitored. Only a small percentage of FcyR^{I^{only}} animals across all experiments demonstrated a mild hypothermia. Table summarises individual values and graphs represent mean \pm SEM. Data is pooled from >4 individual experiments.

Supplementary Figure 4



Supplementary Figure 4: FcγRI^{only} and WT mice are susceptible to thrombocytopenia at a low-dose of platelet-targeting Ab; platelet clearance is partially inhibited by splenectomy but not affected by hemihepatectomy. Circulating platelets were quantified in the blood of (A-B) WT, FcγRI^{only} and FcγR^{null} mice at baseline and after injection of 3μg anti-platelet mAb 6A6, and are represented as (A) percentage over time and (B) number of platelets 4 hours after mAb injection. n=5-6 per group; **** p<0.0001 at 4, 12 and 24 hours. (C-D) Number of platelets in the blood of WT or FcγRI^{only} controls, sham operated, or mice with splenectomy (C) or hemihepatectomy (D), at baseline (1 week after splenectomy or 2 days after hemihepatectomy or sham) and 3,5 hours after 10μg mAb 6A6. (C) n=4-5 per group, data shown from one of two experiments; ** p<0.01. (D) n=3-5 per group, data pooled from two independent experiments; **** p<0.0001.

Supplementary Figure 5



Supplemental Figure 5: mFc γ RI alone is sufficient to mediate mAb therapy of subcutaneous melanoma. Mice were injected subcutaneously with B16-Luc2⁺ melanomas cells with or without therapeutic mAb TA99 treatment and (A,C) tumour growth was monitored by bioluminescent signal 10min after s.c. luciferin injection at indicated timepoints or (B) tumour size measured on day 12. (A) Tumour growth is comparable between untreated WT (triangles, n=5) and Fc γ RI^{only} (circles, n=5 until d7, n=3 at d12) mice. (B-D) Fc γ RI^{only} mice eliminate tumours with TA99 treatment, and Fc γ R^{null} mice do not. (D) Representative photographs taken at day 16. (B-D) correspond to the experiment shown in Figure 2F and are representative of 2 individual experiments.